J. Biochem. **141,** 799–815 (2007)
doi:10.1093/jb/mvm084

Kinetic Studies on the Role of Lys-171 and Lys-358 in the β Subunit of Sarcosine Oxidase from *Corynebacterium* sp. U-96

Mutsumi Saito[1], Miho Kanno[1], Haruo Iizuka[2] and Haruo Suzuki[1,2,*]

[1]Division of Bioscience, Graduate School of Basic Life Science; and [2]Department of Biosciences, School of Science, Kitasato University, Kitasato 1-15-1, Sagamihara, Kanagawa 228-8555, Japan

Received January 30, 2007; accepted March 21, 2007; published online March 29, 2007

Heterotetrameric sarcosine oxidase from *Corynebacterium* sp.U-96(SO-U96) contains non-covalent and covalent flavins. Lys-358 and Lys-171 in the β subunit is present at non-covalent flavin adenine dinucleotide (FAD)- and covalent flavin monodinucleotide (FMN)-binding sites, respectively. The Lys-358 mutant, K358R showed 0.07% activity and higher apparent K_m for sarcosine than the wild-type enzyme, but K358A and K358D mutants showed no activity, suggesting the importance of amino group of Lys358 in the sarcosine-binding to the enzyme. The Lys171 mutants, K171R, K171A and K171D showed 58, 39 and 32% activity of the wild-type enzyme, respectively. An apparent K_m for oxygen and K_d of enzyme–sulphite complex increased by the mutation. The rate of reduction of the FAD of K171 mutants with sarcosine did not change by the mutation. The stopped-flow photodiode array analyses of the anaerobic reduction with sarcosin of the wild-type and K171 mutant enzymes showed characteristic spectra of neutral and anionic semiquinones, especially for K171A enzyme. On the basis of these results, the reductive-half reaction of the wild-type and K171 mutant enzymes is explained by a mechanism involving the semiquinones. Low activity of K171 mutants is suggested to be derived from the low rate of oxidation of the reduced FMN in the enzyme.

Key words: essential lys, flavoenzyme, kinetic mechanism, sarcosine oxidase, site-directed mutagenesis.

Abbreviations: CPR, cytochrome P450 reductase; EDTA, ethylenediaminetetraacetic acid; FAD, flavin adenine dinucleotide; FMN, flavin mononucleotide; IAM, iodeacetamide; IPTG, isopropyl-β-d-thiogalactopyranoside; NAD^+, nicotinamide adenine dinucleotide, oxidized form; PDH, L-proline dehydrogenase; Sar, sarcosine; SO, sarcosine oxidase; SO-ART, SO from *Arthrobacter* sp.1-IN; SO-MAL, SO from *Pseudomonas maltophilia*; SDS-PAGE, sodium dodecylsulphate polyacrylamide gel electrophoresis; SO-PAO, SO from *Pseudomonas aeruginosa* PAO1; SO-P1, SO from *Corynebacterium* sp.P-1; SO-U96, SO from Corynebacterium sp. U-96.

Sarcosine oxidase [SO; sarcosine: oxygen oxidoreductase (demethylating), EC 1.5.3.1] catalyzes the oxidative demethylation of sarcosine to produce formaldehyde, glycine and hydrogen peroxide:

$$CH_3NHCH_2COOH + O_2 + H_2O \rightarrow HCHO + NH_2CH_2COOH + H_2O_2$$

The enzyme has been isolated from various bacterial strains (*1*), and there are three types in its organization, *i.e.*, monomer, heterodimer and heterotetramer. Heterotetrameric SO consists of four non-identical subunits and contains both covalently and non-covalently bound flavins. The enzyme was first purified from *Corynebacterium* sp. U-96 (SO-U96) (*2*), then from various sources, such as *Corynebacterium* sp.P-1 (SO-P1) (*3*), *Arthrobacter ureafaciens* (*4*) and *Arthrobacter* sp.1-IN (SO-ART) (*5*). We have been studying the enzyme from SO-U96 and characterized (*1*, *2*). Chemical modification study of SO-U96 (*6*, *7*) showed that iodoaetamide (IAM) reacts with two lysine residues, one at the sarcosine-binding site and the other at the covalent flavin mononucleotide (FMN)-binding site. Recently, we determined the nucleotide sequences of four subunits of SO-U96, deduced their amino acid sequences, and expressed the enzyme in *Escherichia coli* (*8*). From the sequence of β subunit, we identified the IAM-reactive Lys residues to be K171 and K358 (*7*, *8*). Moreover, we succeeded in the crystallization of the recombinant SO-U96 and in the construction of three dimensional (3D) structure (*9*). The structure shows that K358 presents at the sarcosine-binding site, suggesting its binding with the carboxy anionic ion of sarcosine, and that K171 presents at the oxygen-binding site and in a rather large space (*8*, *9*).

In the present work, to understand the role of these Lys residues in the catalytic reaction, we prepared the mutant enzymes of these Lys residues to Arg, Ala or Asp, and compared their kinetic properties, and their reactivities with sodium sulphite. The K358R mutant, in which Lys358 of β subunit was mutated to Arg, showed very low enzyme activity, and K358A and K358D

*To whom correspondence should be addressed. Tel: +81-42-778-9410, Fax: +81-42-778-9942,
E-mail: suzukih@kitasato-u.ac.jp

mutants showed no activity, confirming the presence of the residue at sarcosine-binding site. The mutation of Lys171 to Arg, Ala or Asp did not lead to serious loss of the enzyme activity. By the analysis of the reductive half-reaction of the wild-type and K171 mutant enzymes, the presence of neutral and anionic semiquinones was indicated with the wild-type and K171 mutant enzymes, though the amount of semiquinones was suggested to be very small with the wild-type and K171R mutant enzymes. The observed rate constants did not change so much with K171R, K171A and K171D mutants, but the reactivity of the enzymes with sodium sulphite was inhibited greatly with these K171 mutants, suggesting that the reactivity of oxygen with the reduced FMN is inhibited by the K171 mutation. This suggests the role of Lys171 in the binding of molecular oxygen to the reduced FMN.

MATERIALS AND METHODS

Materials—His·Bind Resin was from Novagen, DEAE-Sepharose was from Pharmacia/LKB. Isopropyl-β-D-thio-galactopyranoside (IPTG) and X-Gal were from Takara Biochemicals. Quick-Change XL site-directed mutagenesis kit was from Stratagene Corp. Protein markers, Broad range and Kareidoscope were from Bio-Rad. All other chemicals were of the highest grade available.

Bacterial Cells, Plasmids and Culture Conditions—*Escherichia coli* strains, JM109, BL21(DE3) were from Novagen. *Escherichia coli* cells were grown in LB medium, LB agar plate or TP medium. LB: 5 g Bacto-yeast extract, 10 g Bacto-trypton, 8 g NaCl, 2 g Na_2HPO_4, 1 g KH_2PO_4 were dissolved in 1 l H_2O. TP: 15 g Bacto-yeast extract, 20 g Bacto-tryptone, 8 g NaCl, 2 g Na_2HPO_4, 1 g KH_2PO_4 were dissolved in 1 l H_2O, and 1 ml of 0.2 g/ml glucose was added just before use (*10*).

Site-directed Mutagenesis—All common DNA manipulations were performed by standard procedures (*11*). Expression vector for the wild-type enzyme, pSO was prepared from *E. coli* BL21(DE3)/pSO cells (*8*). *In vitro* site-directed mutagenesis of desired residues in the enzyme SO-U96 was carried out by using a Quick-Change XL site-directed mutagenesis kit, following the Instruction Manual (Strategene). The desired mutation was introduced on the wild-type SO-U96 gene in the plasmid pSO using sense and antisense primers. The sequences of sense primers are as follows. 5′-GCCGGCATCGCCCGCCACGACCACGTG for K171R; 5′-GGCATCGCCGCGCACGACCACGTGGC CT-3′ for K171A; 5′-CGCCGGCATCGCCGACCACGACC ACGTG-3′ for K171D; 5′-ACCGGCGGTTTCCGCGGCA CCCCGGGC-3′ for K358R; 5′-ACCGGCGGTTTCGCG GGCACCCCGG GC-3′ for K358A; 5′-GCACCGGC GGTTTCGATGGCACCCCGGGC-3′ for K358D. In the sequence, the underlined indicates the triplet for the mutation. The sequence of antisense primer was complementary to that of the respective sense primer. The *Dpn*I-digested PCR products were then transformed into XL10-Gold ultracompetent cells. The positive colonies on the LB-Ampicillin plate were grown in 5 ml LB medium containing 50 μg/ml Ampicillin at 37°C overnight. The positive colonies were confirmed by sequencing the mutated region. The sequence was determined by Genomic Research Department, Shimadzu–Biotech. The plasmid pSO carrying the desired mutagenic change in the SO-U96 gene was transformed into *E. coli* expression strain BL21 (DE3). To prepare wild-type and mutant SO-U96, *E. coli* cells harbouring plasmids for the wild-type and mutant SO-U96 were cultured, harvested and used to prepare the enzymes as described previously (*8*). The purity of the enzyme was confrmed by SDS–PAGE.

Assay of Enzyme Activity—The activity of enzyme was assayed by measuring the oxygen uptake, using an oxygen electrode (Yellow Springs Instruments, USA) in the presence of various concentrations of sarcosine in 20 mM potassium phosphate buffer (pH 8.0) at 25°C. The concentration of oxygen in the buffer was assumed to be 256 μM at 25°C. The rate(v/e) was expressed as the molar concentration of oxygen consumed per second per molar concentration of enzyme. The concentration (e) of enzyme was determined by measuring the amount of enzyme-bound flavins, assuming that the extinction coefficient of the enzyme-bound flavin is 11.3 $mM^{-1}cm^{-1}$ at 450 nm. The e value is half of the flavin concentration, since the enzyme contains two flavins per molecule. The final concentrations of the wild-type or K171 mutant enzymes were 0.025 to 0.1 μM in the reaction mixture. The higher concentrations were used to assay the activity of K358 mutants.

Spectroscopy—Absorption spectra were measured using a double beam spectrophotometer, type Ubest-50, from Japan Spectroscopic.

Titration of Enzyme with Sodium Sulphite—A spectral change of the enzyme in the visible region by the addition of sodium sulphite was measured in 20 mM potassium phosphate buffer, pH 8.0 at 25°C. Each spectrum was measured at 5 min after addition of sodium sulphite. From the absorbance change at 450 nm, we determined the dissociation constant (K_d) of the enzyme–sulphite complex as described previously (*6*). A solution of sodium sulphite was prepared in ice-cold water just before use.

Stopped-flow Spectroscopy—Rapid reaction kinetic experiments were performed using an Applied Photophysics Stopped-Flow Specrophotometer, 3 × 17 MV, equipped with a HAAKE temperature controller. Time-dependent spectral or absorbance changes were monitored using photodiode array detection or single wavelength detection, respectively. The spectral data were fitted globally by numerical integration methods using Prokin software (Applied Photophysics). The time course of absorbance change at the single wavelength was fit to single or multiple exponential process using a software equipped with the apparatus. Equations used for analyses are presented in the 'Results' section. When it is necessary, anaerobic conditions were attained by the addition of 0.1 μM glucose oxidase, 10 mM glucose and catalytic amounts of catalase to each solution to be mixed. After standing for 60 min at 25°C, the rapid mixing experiments were performed. Before setting solutions to the mixing apparatus, the drive syringes and flow circuit of the apparatus were flushed with the buffer solution containing glucose and

Table 1. **Properties of the wild-type and mutant SO-U96.**

Enzyme preparation	K_m^S, mM[a]	$K_m^{O_2}$, μM[e]	Reaction with sulphite[f]	K_d (mM)		A_{280}/A_{450}	A_{450}/A_{370}
	Sarcosine	Oxygen		Titration	Kinetics		
wild-type	2.76 ± 0.42 (18.5 ± 1.0)	32.9 ± 2.3 (18.9 ± 0.2)	0.213 ± 0.012 0.027 ± 0.003	0.081 ± 0.003	0.13 ± 0.02	16.0	1.09
K171R	1.72 ± 0.15 (9.23 ± 0.25)	31.2 ± 3.0 (9.80 ± 0.2)	0.088 ± 0.003 0.020 ± 0.003	0.373 ± 0.007	0.22 ± 0.04	13.4	0.94
K171A	1.47 ± 0.2 (2.25 ± 0.10)	386 ± 70 (7.4 ± 0.6)	0.021 ± 0.004 0.020 ± 0.010	3.94 ± 0.64	1.43 ± 0.77	17.9	1.03
K171D	2.75 ± 0.44 (2.64 ± 0.16)	730 ± 243 (6.1 ± 1.2)	0.0074 ± 0.001 0.025 ± 0.004	3.53 ± 0.24	3.4 ± 1.1	9.36	1.06
K358R[b]	17.4 ± 0.8 (0.0113 ± 0.0003)			0.054 ± 0.014		19.8	1.05
K358A[c]	n.d.			0.068 ± 0.001		24.4	1.1
K358D[d]	n.d.			0.073 ± 0.002		35	0.98

[a]K_m^S was determined in the air-saturated buffer (256 μM O_2), and the apparent k_{cat} (s^{-1}) values are shown in parentheses. The final concentrations of enzyme were [b]1.5 μM, [c]2 μM and [d]1 μM in the assay mixure. [e]$K_m^{O_2}$ was determined in the presence of 20 mM sarcosine, and the apparent k_{cat} (s^{-1}) values are shown in parentheses. These values were determined for the wild-type and K171R mutant enzymes in the presence of 40–850 μM oxygen. [f]The rate constants for the formation and the dissociation of enzyme–sulphite complex obtained by the stopped flow method. The values in the upper line is k_{+1} ($mM^{-1}s^{-1}$) and the lower line k_{-1} (s^{-1}). n.d., not detected.

glucose oxidase. Nitrogen gas was gently purged between the plunger and barrel of the drive syringe during the mixing experiments.

RESULTS

Effect of Site-directed Mutation on the Activity of Enzyme—We reported that K358 and K171 in the β subunit of SO-U96 is specifically modified by IAM in the presence or absence of sodium acetate, and proposed that K358 and K171 were at non-covalent and covalent flavin-binding site, respectively (*6*, *7*). We also reported that covalent FMN binds with sulphite and that the K_d of the enzyme–sulphite complex increases with the IAM-modification of K171 (*6*). The results indicate that the modification of K171 induces conformational changes around covalent FMN to reduce the association of sulphite with the FMN. Electrons are believed to be transferred in the native enzyme (*1*, *3*, *12–14*) as,

step	1		2		3	
sarcosine	→	non-covalent FAD	→	covalent FMN	→	molecular oxygen

Scheme. 1.

We proposed that by IAM-modification of K171 the main path of electrons from sarcosine to oxygen becomes, sarcosine → non-covalent flavin adenine dinucleotide (FAD) → molecular oxygen (*6*). To clarify that the proposal is correct or not, and to understand the role of these residues in catalysis, we generated three mutants for each residues, K171R, K171A, K171D, K358R, K358A and K358D, as described in 'Materials and Methods'. The purity of the wild-type and mutant enzymes prepared was confirmed by the SDS–PAGE (data not shown). The yields of mutant enzymes were comparable to that of the wild-type enzyme, and the spectral properties were similar in these proteins (Table 1). Using these enzyme preparations, we determined their kinetic parameters of overall reaction.

As shown in Table 1, K358R mutant showed approximately 10^{-3} times activity of the wild-type enzyme, and an apparent K_m for sarcosine was six-time higher than the wild-type enzyme. The other mutants, K358A and K358D, showed no activity with rather high concentrations of the enzyme (Table 1). Our crystallographic studies of SO-U96 showed that the carboxy group of dimethylglycine is bound to the amino group of K358 (*9*), so it is conceivable that the carboxy oxygen of sarcosine is hydrogen-bonded with the amino hydrogen of K358, which amino group has p*K*a 6.7 (*7*) and is not protonated under the experimental conditions(pH 8.0). K358R mutant had very low activity with high K_m, indicating that the change from amino to guanidium group changes the orientation and strength of the hydrogen bond. That is, K358 determines the fine orientation of substrate, sarcosine, at the active site of enzyme.

To see if mutation of K171 adjacent to the covalent FMN-binding H172 affects the affinity of sarcosine to the enzyme, the activity of enzyme was measured at various concentrations of sarcosine. The K171R, K171A and K171D mutants showed 1/2 to 1/3 activity of the wild-type enzyme at the saturating concentrations of sarcosine and oxygen (Fig. 1A, Table 1), but an apparent K_m for sarcosine was almost constant with these mutants, indicating no change in the affinity of sarcosine to these enzyme. This is quite reasonable, since K171 presents at the oxygen-binding site, but not at the sarcosine-binding site (*6*, *7*, *9*). Moreover, the results indicate that the K171 mutants do not show the fatal defect in the function of enzyme.

The side chain of K171 faces the tunnel from the isoalloxazine ring of FMN to the surface of the enzyme protein [(*9*), Fig. 2]. It is conceivable that molecular oxygen has access from the outside of the enzyme protein to the covalent FMN through the tunnel. This gives us an idea that the affinity of oxygen with the covalent FMN may change with the K171R, K171A and K171D mutants. To examine this, the rate of oxidation of

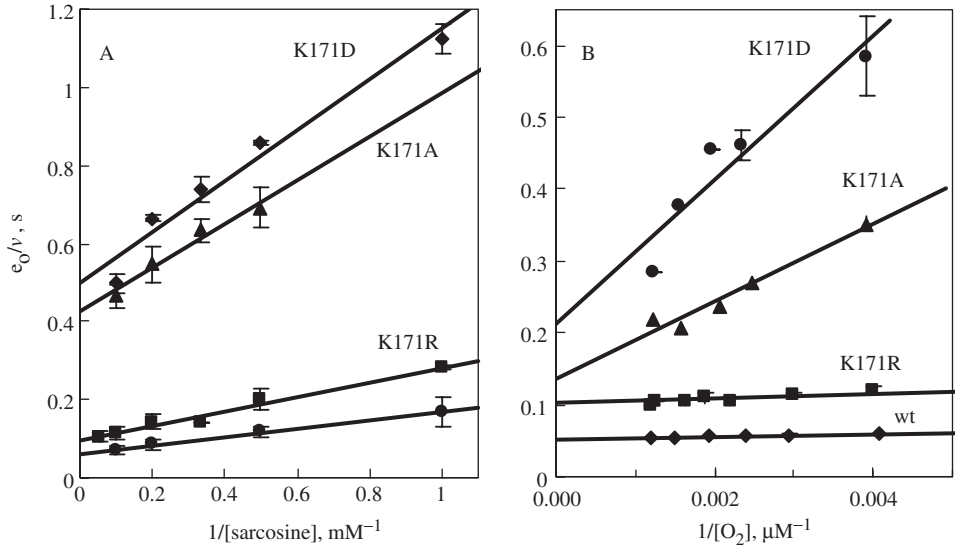

Fig. 1. **Effect of concentrations of sarcosine (A) and oxygen (B) on the rate of oxidation of sarcosine with the wild-type and K171 mutant SO-U96.** The rate of reaction was determined by measuring the oxygen uptake at 25°C, pH 8.0 as described in 'Materials and Methods'. Enzymes used were wild-type (filled circle), the mutants K171R (filled square), K171A (filled triangle) and K171D (filled diamond). (A) Plot of e_0/v versus 1/[sarcosine]. The final concentration of enzyme used was 0.05 μM (wild-type), 0.06 μM (K171R mutant) and 0.075 μM (K171A and K171D mutants). The concentration of oxygen was 256 μM. (B) Plot of e_0/v versus 1/[O_2]. The final concentration of enzyme used was 0.1 μM (wild-type), 0.15 μM (K171R mutant), 0.2 μM (K171A mutant) and 0.3 μM (K171D mutant). The concentration of sarcosine used was 20 mM.

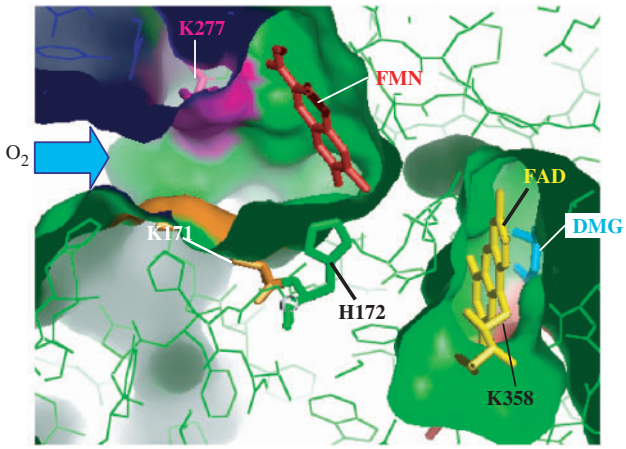

Fig. 2. **A surface view of the access of oxygen to covalent FMN in SO-U96 (PDB accession code, 1X31).** Large arrow shows the route of oxygen from the outside of the enzyme protein. K171, orange; H172, green; K358, red; FMN, red; FAD, yellow; K277, purple; DMG (dimethyl glycine), magenta; α-subunit, blue; β subunit, green. Figure was produced by using PyMol(http://pymol.sourceforge.net/).

sarcosine was determined at various concentrations of oxygen in the presence of sufficient concentration of sarcosine. As Fig. 1B shows, the rate obtained with the wild-type and K171R mutant enzymes showed low dependency on the oxygen concentration, but those with the K171A and K171D mutants showed highly dependent on the oxygen concentration. That is, an apparent K_m for oxygen changed greatly with the mutation of Lys171 to Ala or Asp (Table 1). The results suggest that K171 has some role in the binding of oxygen with enzyme.

Titration of the Enzyme with Sodium Sulphite—The reactivity of free flavins and flavoproteins with sulphite was studied well (*15*, *16*). Massey *et al.* (*16*) observed that there is correlation between sulphite and oxygen reactivity of flavoproteins. This led to the experiments by Jorns (*13*) and then by us (*6*) that covalent FMN of SO specifically reacts with sulphite. Therefore, we tested if the mutation of Lys171 to Arg, Ala or Asp affects the reactivity of the covalent FMN to sulphite, since the K171 mutants showed the difference in an apparent K_m for oxygen (Table 1). The enzyme was titrated with sodium sulphite and the K_d of the enzyme–sulphite complex was determined. Figure 3 shows the spectral changes of the enzyme by the addition of sodium sulphite. The spectral change of the wild-type enzyme was similar to that of K171R, and that of K171A is similar to that of K171D. This indicates that micro-environments around isoalloxazine ring of covalent FMN changed slightly by mutation to Arg, but largely by mutation to Ala and Asp. This can be shown quantitatively by determining K_d of enzyme–sulfite compound. From the absorbance change at 450 nm, K_d was determined by the plot, [sulphite]/ΔA_{450} versus [sulphite] (*6*). K_d shown in Table 1 was determined by 3–10 titrations for each enzymes. As expected, K_d value changed greatly by mutation. This is reasonable, since the covalent FMN of the enzyme is bound to H172, next to the residue mutated. By plotting logK_d against log apparent $K_m^{O_2}$ (Fig. 4), a linear relationship was observed. Though $K_m^{O_2}$ is an apparent K_m for oxygen, Fig. 4 indicates that sulphite affinity of enzyme is strongly related to the oxygen affinity of enzyme.

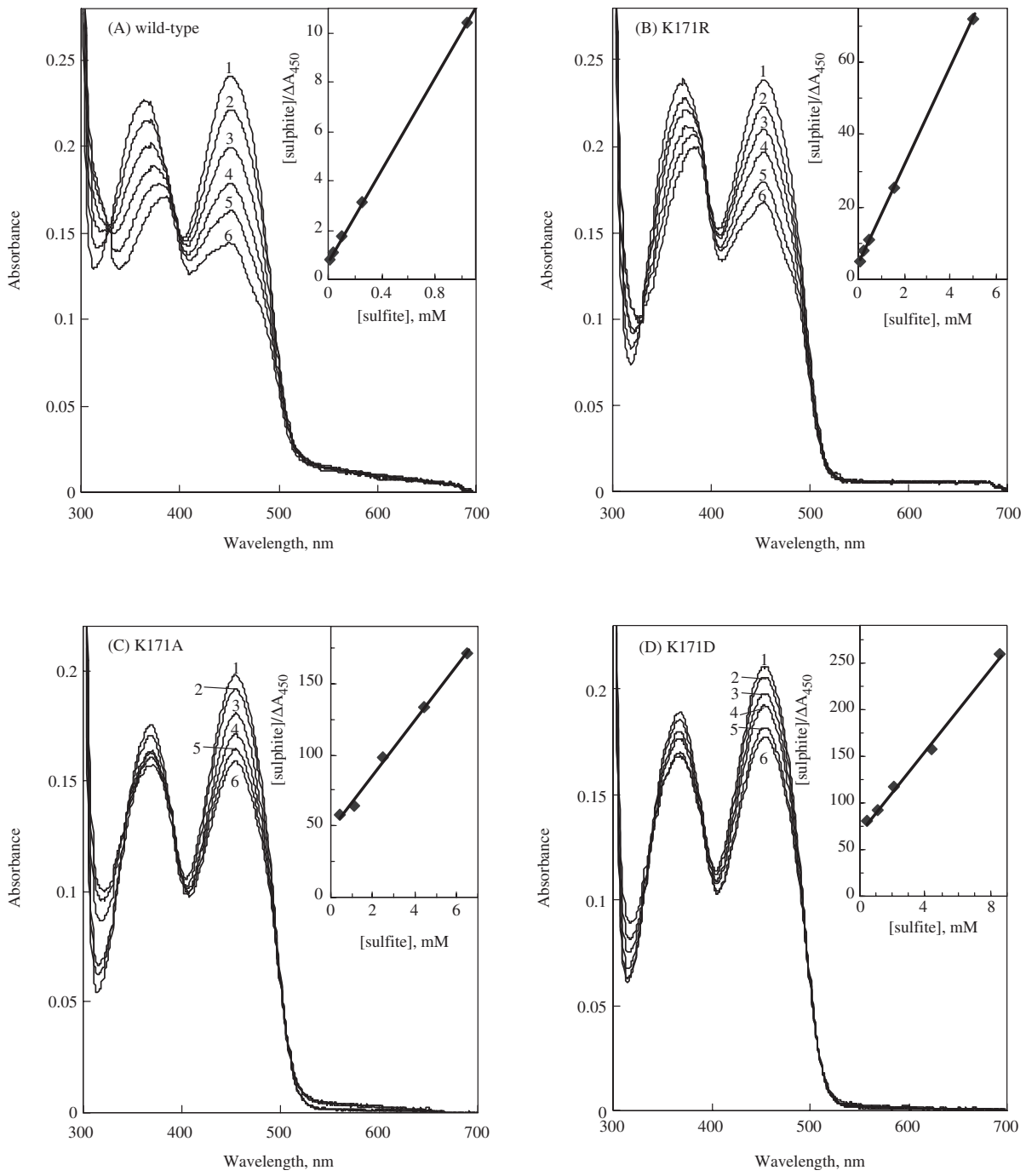

Fig. 3. **Titration of sarcosine oxidase with sodium sulphite.** Enzymes used were wild-type (A), the mutants K171R (B), K171A (C) and K171D (D). Curve 1 was the initial spectrum of enzyme in 20 mM potassium phosphate buffer, pH 8.0, at 25°C. Curves 2–6 were the spectra obtained at 5 min after each addition of sodium sulphite; 0.01, 0.03, 0.10, 0.25, 1.04 mM in (A), 0.10, 0.24, 0.44, 1.53, 5.03 mM in (B), 0.4, 1.1, 2.5, 4.4, 6.5 mM in (C) and 0.4, 1.1, 2.1, 4.4, 8.6 mM in (D), respectively. Each spectrum was corrected for the volume change by the addition of sodium sulphite. The inset shows a plot [sulphite]/$\Delta A_{450\ nm}$ versus [sulphite] (*6*). From the plots, the dissociation constants were determined.

We also determined K_d of the enzyme–sulphite complex using K358 mutants (Table 1). The mutants showed K_d values (54–73 μM) similar to that of the wild-type enzyme. This indicates that these mutation of K358 does not affect the binding of the covalent FMN to sulphite. That is, the environment of the covalent FMN does not change by the K358 mutation, though the K358 mutation affected greatly on the catalytic activity of enzyme (Table 1). As K358 mutants had a low enzyme activity, we did not study further on these mutants.

Kinetics of the Reductive-half Reaction in the Presence of Sodium Sulphite—The overall reaction is composed of

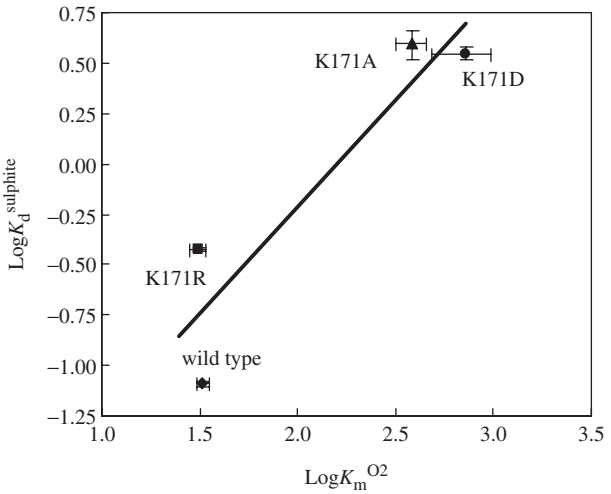

Fig. 4. **Plot of log $K_d^{sulphite}$ versus log[apparent $K_m^{O_2}$].** The data in Table 1 were used to plot. The dissociation constants (K_d) of enzyme–sulphite complex were determined as described in Fig.3 and apparent $K_m^{O_2}$ values were determsined as described in Fig.1B.

electron transfer steps from sarcosine to oxygen (Scheme 1). So, in the present study, we analysed each step kinetically by our stopped-flow instrument. As previously reported (*12*), the reaction mechanism of SO-U96 is complex even the reductive half-reaction. This is because the enzyme contains two flavin prosthetic groups with different role. That is, the non-covalent FAD reacts with substrate sarcosine, and the covalent FMN reacts with oxygen (*1*). So, to simplify the analysis of the reaction, we monitored the reduction of the FAD in the presence of 40 mM sodium sulphite to inactivate the covalent FMN (*6*, *12*, *17*). At this sodium sulphite concentration, 99% of the FMN moiety of the wild-type and K171R mutant enzymes is calculated to be in the complex with sulphite, but nearly 90% of K171A and K171D enzymes is in the complex with sulphite, using K_d of enzyme–sulphite complex (Table 1). Then, the reoxidation of the reduced enzymes is expected to be suppressed in the presence of sufficient concentrations of sodium sulphite. Usefulness of the sulphite-treatment of enzyme has been shown by using the tetrameric SO from SO-ART (*17*).

Figure 5A-1 shows the spectral changes of the wild-type and mutant enzymes detected by the photodiode array stopped-flow spectroscopy after mixing the oxidized form of enzyme with 5 mM sarcosine in the presence of 40 mM sodium sulphite. The spectral data were fitted globally using numerical integration methods using Prokin software (Applied Photophysics). Data collected over 10 s after mixing were fit to a two-step model (*17*).

$$A \rightarrow B \rightarrow C$$

The species A represents the oxidized form of sulphite-bound SO-U96 (Fig. 5A-1 inset). The calculated spectral form B indicates the 2-electron reduced FAD of the sulphite-bound SO-U96. Species C is slowly formed, and meaning of this change is not known. Experiments similar to Fig. 5A were performed using the K171R mutant enzyme (Fig. 5B-1). Inset in Fig. 5B shows the calculated spectral changes, and the changes are similar to that of the wild-type enzyme. That is, the fast change from the form A to B, and the slow change from the form B to C. The spectra observed during reduction were similar in the wild-type and mutant K171R enzymes, indicating the structural similarity around the FAD isoalloxazine ring of the wild-type and K171R mutant enzymes.

Similar experiments as above were performed using the K171A and K171D mutant enzymes. As in the case of the wild-type and K171R mutant enzymes, the spectral changes after mixing the enzyme with sarcosine indicates that the oxidized form of FAD (enzyme species A) rapidly changed to the enzyme species B, which slowly changed to the other species C as shown in Fig. 5C-1 and D-1. The initial fast phase is assumed to be the change of the oxidized form of FAD to the reduced one. In the case of K171A and K171D enzymes, long wavelength species slowly appeared. This must be a semiquinoid species derived from the electron transfer from the reduced $FADH_2$ to FMN, to which sulphite is not bound. To see if this idea is correct or not, similar experiments were performed in the presence of 100 mM sodium sulphite, where 96% of FMN in the K171A and K171D enzymes is calculated to be bound with sulphite. Compared with the spectra obtained in the presence of 40 mM sodium sulphite, the absorbance in the long wavelength region was decreased (data not shown), supporting the idea. The rate of slow appearance of long wavelength species was estimated to be very low ($0.5 s^{-1}$), and too slow to explain the overall rate. Therefore, we did not consider this further, and the initial fast phase was analysed.

Panels A-2, B-2, C-2 and D-2 in Fig. 5 show the initial rapid phase of absorbance decrease at 450 nm after mixing the enzyme with 5 mM sarcosine in the presence of 40 mM sodium sulphite. The fast phase was well fitted by one exponential process (Fig. 5A-2 and B-2) and one or two exponential process (Fig. 5C-2 and D-2) (Equation 1).

$$A_{450} = C_1 \exp(-k_{obs1}t) + C_2 \exp(-k_{obs2}t) + b \qquad (1)$$

where k_{obs1} and k_{obs2} are the observed rate constants for the fast and slow phases, C_1 and C_2 are the relative amplitude value for the fast and slow phases, respectively, and b is an offset value to account for a non-zero base line.

Though the time course was fitted by two exponential process for the K171A and K171D enzymes, we considered the fast phase only, since these enzymes contain the sulphite-unbound FMN and the slow phase must be derived from the formation of semiquinoid species by one electron transfer from $FADH_2$ to this FMN species (Fig. 5C-1 and D-1). Similar experiments were performed at various concentrations of sarcosine. A reciprocal of the apparent first order rate constant (k_{obs1}) of the fast phase is plotted against that of sarcosine concentration (Fig. 6). A linear relationship showed a fixed intercept on the ordinate, indicating that a Michaelis complex is formed

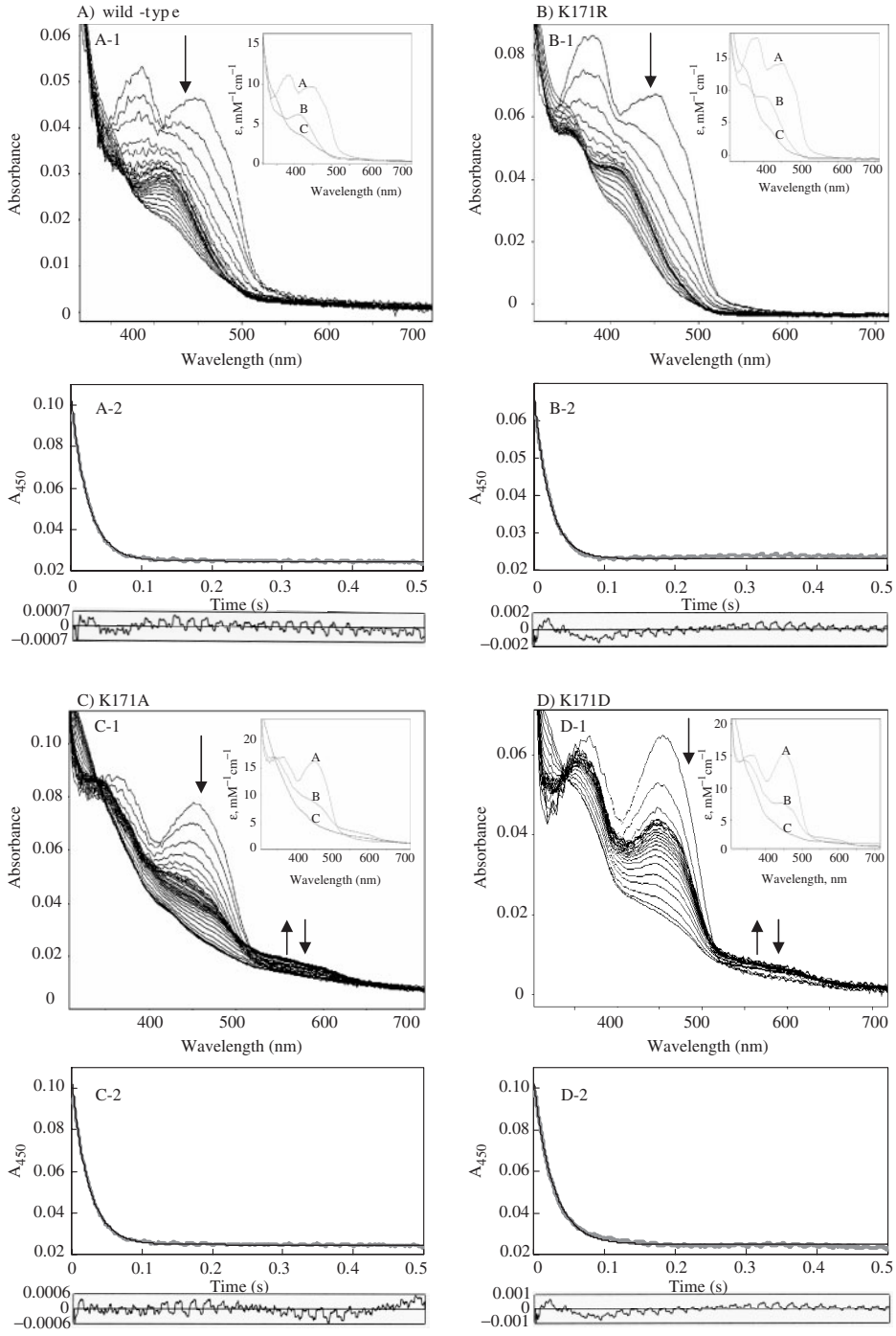

Fig. 5. **Reduction of the flavin moiety of the wild-type and mutant SO-U96 after mixing with 5 mM sarcosine in the presence of 40 mM sodium sulphite.** A-1, B-1, C-1 and D-1, time dependent spectral change were monitored for 1.28 ms to 10 s after mixing the enzyme with sarcosine by the stopped-flow photodiode array spectroscopy. For clarity, only selected spectra are shown. Arrows indicate the direction of observed spectral change. Conditions (after mixing): 50 mM potassium phosphate buffer, pH 8.0, 5.0 μM enzyme at 25°C. Inset: deconvoluted spectra for the long time reaction(10 s) were fitting to two step model, A → B → C. Spectrum A, wild-type and mutants species in the presence of 40 mM sodium sulphite; spectrum B, enzyme species following the fast phase of the reductive half-reaction and spectrum C, enzyme species following the slow phase of the reductive half-reaction. The rate constant (s^{-1}) obtained from global fitting are, wild-type enzyme (A-1): 42.8 ± 0.4, 0.78 ± 0.01, K171R mutant (B-1): 39.6 ± 0.2, 0.37 ± 0.01, K171A mutant (C-1): 43.6 ± 0.3, 0.23 ± 0.01, K171D mutant (D-1): 40.1 ± 0.3, 2.1 ± 0.0 for steps A → B → C, respectively. A-2, B-2, C-2, D-2: Reduction of wild-type and K171 mutant enzymes by sarcosine in the presence of 40 mM sodium sulphite was monitored by single-wavelength stopped-flow spectroscopy monitored for 0.5 ms. Transient obtained at 450 nm illustrating the monophasic (A-2, B-2) or biphasic(C-2, D-2) nature of the reductive transient observed at this wavelength. The thick lines represent the data points and the thin lines are the fit to the data point.

before reduction of non-covalent FAD of the enzyme (Scheme 2).

$$E^{ox} + Sar \overset{K_d}{\rightleftharpoons} E^{ox} \cdot Sar \xrightarrow{k_{obs1/max}} E^{red} + P$$

Scheme. 2.

In the scheme, E^{ox} and E^{red} represent the oxidized and reduced forms of the enzyme FAD, respectively, and Sar represents sarcosine.

Data were fitted to obtain K_d and $k_{obs1/max}$ values using the following equation.

$$k_{obs1} = k_{obs1/max}[Sar]/(K_d+[Sar]) \quad (2)$$

where K_d is the dissociation constant of enzyme–sarcosine complex, and k_{obs1} and $k_{obs1/max}$ are the rate constant observed and the maximum rate of reduction, respectively.

As Fig. 6 shows, the reciprocal of k_{obs1} values obtained with the wild-type, K171R, K171A and K171D mutant enzymes were on the almost same line, indicating that the reactivity of the enzyme FAD with sarcosine does not change by these K171 mutation. From the plot, the limiting value of k_{obs1}, $k_{obs1/max}$ was determined to be $145.9 \pm 5.3\,s^{-1}$, and the dissociation constant of enzyme–sarcosine complex, K_d was 11.9 ± 0.8 mM (Table 2). This indicates that the reduced activity of the K171 mutants is derived from the reduced rate at the step 2 and/or 3 in the electron transfer from sarcosine to oxygen (Scheme 1). To clarify this, the reductive half-reaction of the flavin prosthetic groups was analysed by the stopped-flow method under anaerobic conditions without added sodium sulphite.

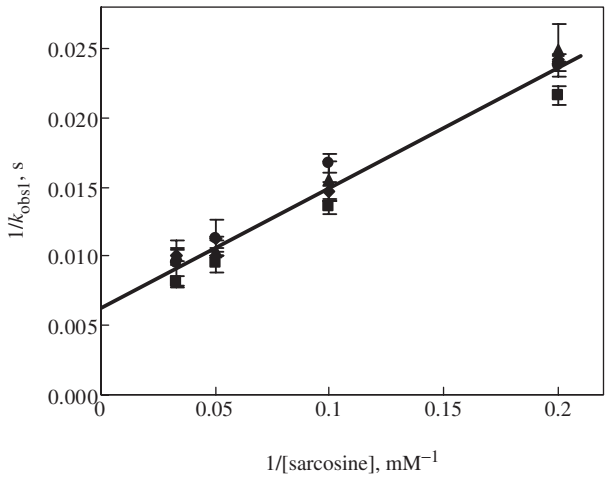

Fig. 6. **Effect of concentration of sarcosine on the rate of reduction of the wild-type and mutant enzymes.** Double reciprocal plot of the observed rate constants (k_{obs1}) versus sarcosine concentration. Apparent rate constant (k_{obs1}) was obtained from time-courses of the decrease in absorption at 450 nm as described in Fig. 5. Enzymes used were the wild-type (filled diamond), and the K171R (filled square), K171A (filled triangle), and K171D (filled circle) mutant enzymes.

Kinetics of Reductive Half-reaction Under Anaerobic Conditions—Figure 7 shows the spectral changes of the wild-type and K171 mutant enzymes detected by photodiode array stopped-flow spectroscopy. The wild-type enzyme rapidly changed to one spectral species, then the species slowly changed to another species (Fig. 7A-1). Similar spectral change was observed with the K171R mutant (Fig. 7B-1). These spectral changes can be explained by using our proposed scheme [(*12*), Scheme 3], since a spectrum indicating the presence of neutral flavin semiquinone was not observed clearly during reduction. But slight absorbance change at 500–700 nm region might suggest the formation of a small amount of neutral semiquinone. Moreover, it is reasonable to think that electron transfer between redox prosthetic groups occurs one electron at a time (*18*). Therefore, we modified the mechanism proposed (*12*) as shown in Scheme 3. That is, step 1: the oxidized form of the enzyme FAD is reduced by sarcosine, step 2: the electrons rapidly transfer from the reduced FAD to the oxidized FMN to reform the oxidized FAD, by forming semiquinoid species, step 3: the oxidized FAD is reduced again by sarcosine (Scheme 3).

$$E^{ox}_{ox} \overset{Sar}{\rightleftharpoons} E^{ox}_{ox}\cdot Sar \xrightarrow{k_{+2}} E^{red}_{ox} \xrightarrow{k_{+3}} E^{sq}_{sq} \xrightarrow{k_{+4}} E^{ox}_{red} \overset{Sar}{\rightleftharpoons} E^{ox}_{red}\cdot Sar \xrightarrow{k_{+5}} E^{red}_{red}$$

Scheme. 3.

where E^{ox}, E^{sq} and E^{red} represent the oxidized, semiquinoid and reduced forms of the enzyme FAD, respectively, and E_{ox}, E_{sq} and E_{red} represent the oxidized, semiquinoid and reduced forms of the enzyme FMN, respectively. Then the rate of reduction of the enzyme flavin was analysed by measuring the absorbance change at 450 nm (Fig. 7A-2). The absorbance decrease was fitted with two exponential process (Equation 1). The rates were determined at various concentrations of sarcosine, and the maximum rate and apparent K_d obtained are shown in Table 2.

Table 2. **Kinetic Parameters for Reductive Half-reaction of wild-type and mutant SO-U96.**

Enzyme	Wavelength[a]	$k_{obs1/max}$ (s^{-1}) ($K_{d/obs1}$ [mM])	$k_{obs2/max}$ (s^{-1}) ($K_{d/obs2}$ [mM])	$k_{obs3/max}$ (s^{-1}) ($K_{d/obs3}$ [mM])
Wild-type	450	59.2 ± 1.1 (1.91 ± 0.15)	3.96 ± 0.17 (3.75 ± 0.74)	
K171R	450	100.5 ± 2.5 (8.09 ± 0.49)	4.72 ± 0.66 (25.7 ± 5.7)	
K171A	450	121.6 ± 9.7 (11.2 ± 1.9)	21.9 ± 1.5 (n.d.)	4.40 ± 0.88 (n.d.)
K171D	450	76.7 ± 2.4 (6.0 ± 0.49)	13.2 ± 1.7 (22.5 ± 4.6)	0.44 ± 0.02 (6.0 ± 0.8)
K171A	550	24.4 ± 2.1 (n.d.)	6.3 ± 2.0 (127 ± 44)	
K171D	550	33.3 ± 3.1 (6.3 ± 1.7.)	8.7 ± 1.1 (15.5 ± 3.7)	

[a]Wavelength (nm) used to collect the stopped-flow data. The parameters were calculated from the data shown in Fig. 8 (450 nm) and Fig. 9 (550 nm). n.d., not determined.

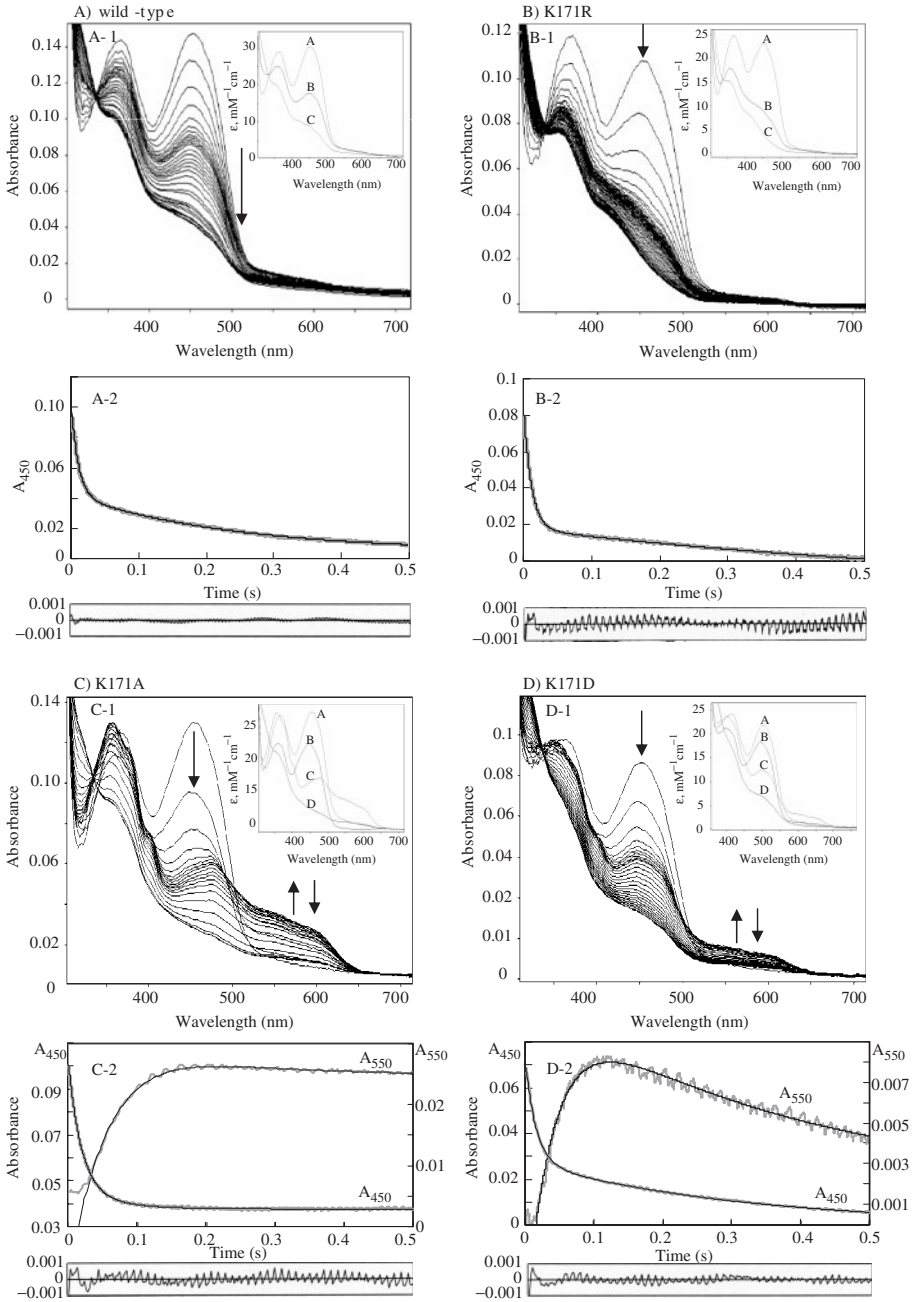

Fig. 7. **Reduction of the wild-type and K171 mutant SO-U96 with 5 mM sarcosine under anaerobic conditions.** Spectral change was monitored by the stopped-flow photodiode array spectroscopy. Conditions(after mixing); 50 mM potassium phosphate buffer, pH 8.0, 5.0 μM enzyme at 25°C. Enzyme used was the wild-type (A), the K171R (B), K171A (C) and K171D (D) mutant enzymes. A-1, B-1 and D-1: Time dependent spectral changes were monitored for 1.28 ms to 10 s after mixing, and C-1 was monitored for 1.28 ms to 50 s. For clarity, only selected subsequent spectra are shown. Inset: deconvoluted spectra for the wild-type and K171R enzymes were fitting to a two-step model, A → B → C. Spectrum A, the oxidized form of the wild-type and K171 mutant enzymes; spectrum B, enzyme species following the fast phase of the reduction and spectrum C, enzyme species following the slow phase of the reduction. The rate constants (s^{-1}) obtained from global fitting were as follows, wild-type (A-1); A → B, 46.4 ± 0.02, B → C, 1.75 ± 0.01. K171R (B-1); A → B, 43.7 ± 0.2, B → C, 1.3 ± 0.003. The deconvoluted spectra of K171A (C-1) and K171D mutant (D-1) were fitting to a three-step model, A → B → C → D. The rate constant (s^{-1}) for steps; A → B, 52.9 ± 0.4, B → C, 25.9 ± 0.1; C → D, 0.31 ± 0.0 (s^{-1}) for K171A mutant, and A → B, 72.9 ± 1.9, B → C, 41.1 ± 0.4, C → D, 1.2 ± 0.0 for K171D mutant. A-2, B-2, C-2, and D-2, The absorbance change of enzyme was monitored at 450 nm. The thick lines represent the data points and the thin lines are the fit to the data point analysed by using the software equipped with the stopped-flow instrument. The time courses were well fitted by two exponential process (wild-type and K171R), or three exponential process (K171A and K171D). The thick lines represent the data points and the thin lines are the fit to the data point by using the software equipped with the apparatus. C-2, D-2: transient obtained at 550 nm is also shown for K171A (C-2) and K171D (D-2). The thick lines represent the data points and the thin lines are the fit to the data point analysed by using the software equipped with the instrument.

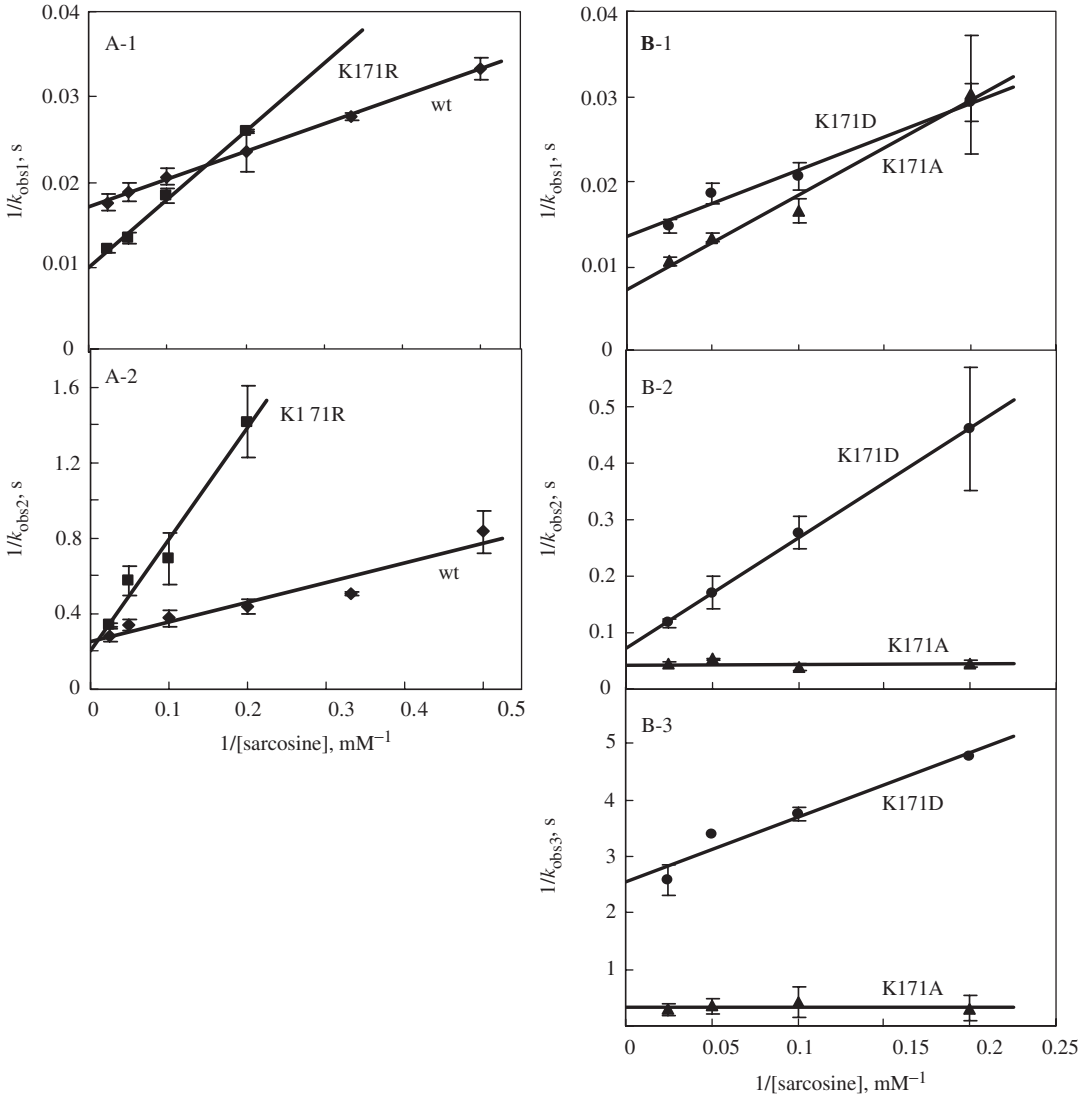

Fig. 8. **Effect of concentration of sarcosine on the rate of reduction of the wild-type and mutant SO-U96.** Double-reciprocal plot of the observed rate constants (k_{obs1}, k_{obs2} and k_{obs3}) versus sarcosine concentration. Enzymes used were wild-type (filled diamond), the mutants K171R (filled square), K171A (filled triangle) and K171D (filled circle).

The K171A and K171D mutant enzymes showed a spectral change different from those of the wild-type and K171R mutant enzymes (Fig. 7C and D). The oxidized form of K171A must be changed fast to the half-reduced form, then to a long wavelength-absorbing species, and very slowly to the fully reduced form. Both K171A and K171D mutants showed spectra indicating a presence of semiquinones as proposed by Ali *et al.* [(*19*), Fig. 7C-1 and D-1]. That is, the spectra observed during reduction showed characteristic spectra of neutral and anionic semiquinones. Therefore, reduction of K171A and K171D mutants with sarcosine can be explained by Scheme 4, modifying the scheme of Ali *et al*. (*19*).

$$\mathbf{E}_{ox}^{ox} \overset{Sar}{\rightleftharpoons} \mathbf{E}_{ox}^{ox}\cdot\mathbf{Sar} \xrightarrow{k_{+2}} \mathbf{E}_{ox}^{red} \xrightarrow{k_{+3}} \mathbf{E}_{sq}^{sq} \overset{Sar}{\rightleftharpoons} \mathbf{E}_{sq}^{sq}\cdot\mathbf{Sar} \xrightarrow{k_{+4}} \mathbf{E}_{red}^{red}$$

Scheme. 4.

In Scheme 4, $\mathbf{E}_{ox}^{ox}$, $\mathbf{E}_{ox}^{red}$, $\mathbf{E}_{sq}^{sq}$ and E_{red}^{red} represent the oxidized, the FAD-reduced, the flavin semiquinone and the fully reduced form of enzyme, respectively.

Single-wavelength stopped-flow studies were performed at 450 nm to analyse the substrate dependence of the individual step seen in the photodiode array experiments. Though the spectral changes of K171A enzyme were different from those of K171D enzyme (Fig. 7D-1), a time course of absorbance change of K171A and K171D at 450 nm was similar to each other (Fig. 7C-2 and D-2). The absorbance decrease was well fitted with the triple exponential expression using the software equipped with the stopped-flow apparatus.

$$A_{450}=C_1\exp(-k_{obs1}t)+C_2\exp(-k_{obs2}t)+C_3\exp(-k_{obs3}t)+b \quad (3)$$

where k_{obs1}, k_{obs2} and k_{obs3} are the observed rate constants for the fast, intermediate and slow phases,

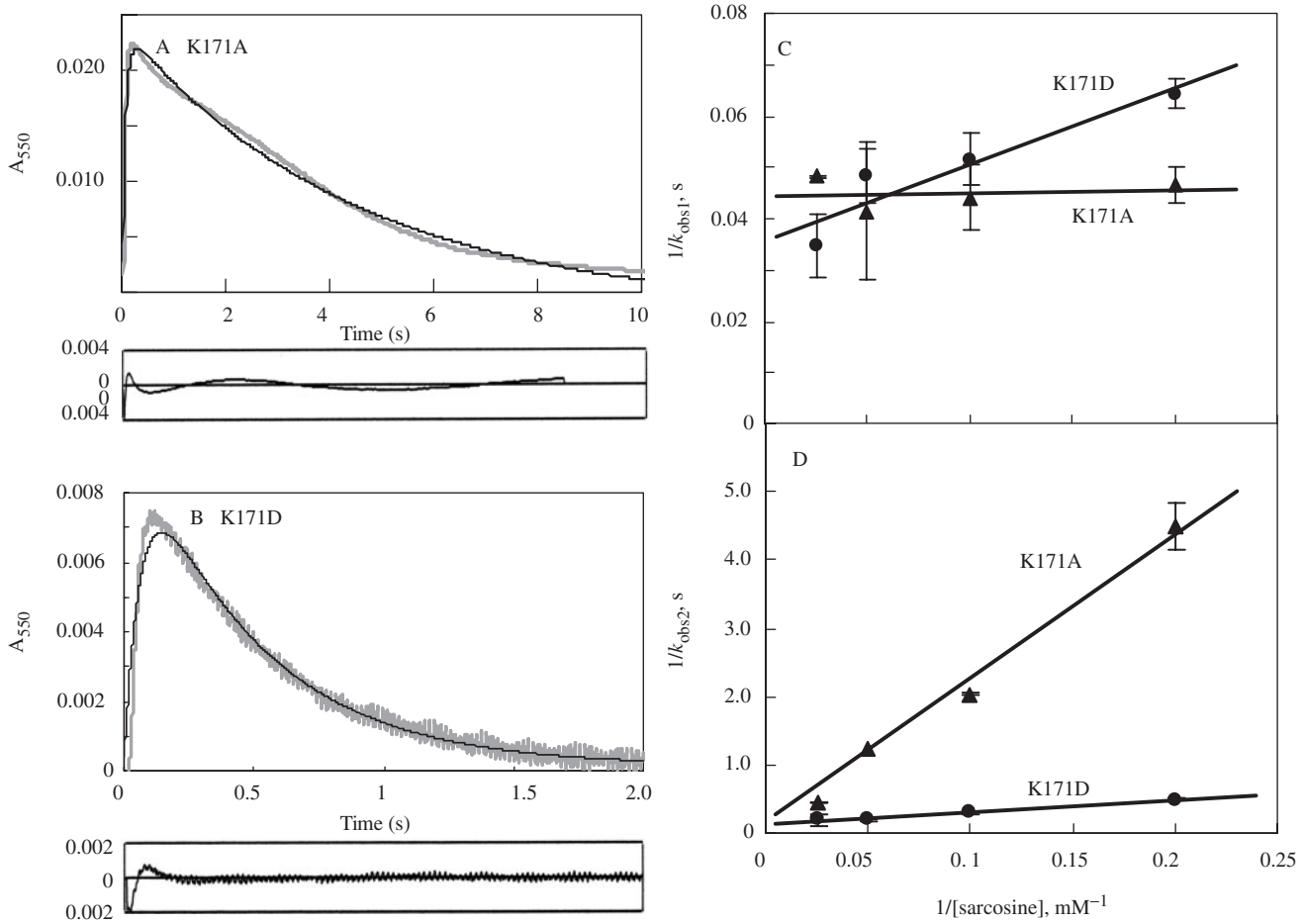

Fig. 9. **Stopped-flow traces at 550 nm after mixing the mutant enzymes (K171A, K171D) with 5 mM sarcosine under anaerobic conditions.** Conditions (after mixing); 50 mM potassium phosphate buffer, pH 8.0, 5.0 μM enzyme at 25°C. Enzymes used were K171A(A) and K171D(B). The thick lines represent the data points and the thin lines are the fit to the data point analysed by using the software equipped with the instrument. (A) The time course of reduction of K171A mutant with 5 mM sarcosine was fitted by two exponential process. The observed rate constants for the fast 'up' (k_{obs1}) and 'down' (k_{obs2}) phases are 19.1 and 0.22 s^{-1}. (B) The time courses of reduction of K171D mutant with 5mM sarcosine was fitted by two exponential process. The observed rate constants for the fast 'up' (k_{obs1}) and 'down' (k_{obs2}) phases are 17.8 and 1.8 s^{-1}. (C, D) Double reciprocal plot of the observed rate constants [k_{obs1} (C) and k_{obs2} (D)] versus sarcosine concentration. Sarcosine concentrations were 5.0, 10, 20 and 40 mM. Enzymes used were the mutants K171A (filled triangle) and K171D (filled circle).

respectively, C_1, C_2 and C_3 are the relative amplitude values for three phases, and b is an offset value to account for a non-zero base line. The k_{obs} values obtained were plotted against the concentrations of sarcosine (Fig. 8), and the rates at limiting substrate concentrations and apparent K_d were obtained (Table 2). The appearance of long wavelength species was clearly shown for the K171A and K171D mutant enzymes (Fig. 7C-2 and D-2), so we monitored the absorbance change at 550 nm during the reductive half-reaction (Fig. 9). After a short lag phase, the absorbance increased, then slowly decreased. These absorbance change was fitted by Equation 4.

$$A_{550} = \{k_{obs1}/(k_{obs2} - k_{obs1})\}C \{\exp(-k_{obs1}t) - \exp(-k_{obs2}t)\} + b \quad (4)$$

where k_{obs1} and k_{obs2} are the observed rate constants for the formation and decay of the semiquinoid intermediate respectively. C is the amplitude term, and b is an off-set value. The values, k_{obs1} and k_{obs2} obtained at various concentrations of sarcosine were plotted as shown in Fig. 9C, D. The limiting value, $k_{obs1/max}$ value agreed with $k_{obs2/max}$ determined by monitoring the absorbance change at 450 nm (Table 2). This suggests that the intermediate phase observed at 450 nm is the step to form the semiquinoid species, we will consider this point further in the 'DISCUSSION' section.

Comparing the observed rate constants of the mutant enzymes with those of the wild-type enzyme (Tables 1 and 2), the reductive-half reaction was not inhibited by the mutation of K171 to R, A and D. It is therefore suggested that the rate of oxidation of the reduced FMN with oxygen must be inhibited by the mutation of K171 to R, A and D.

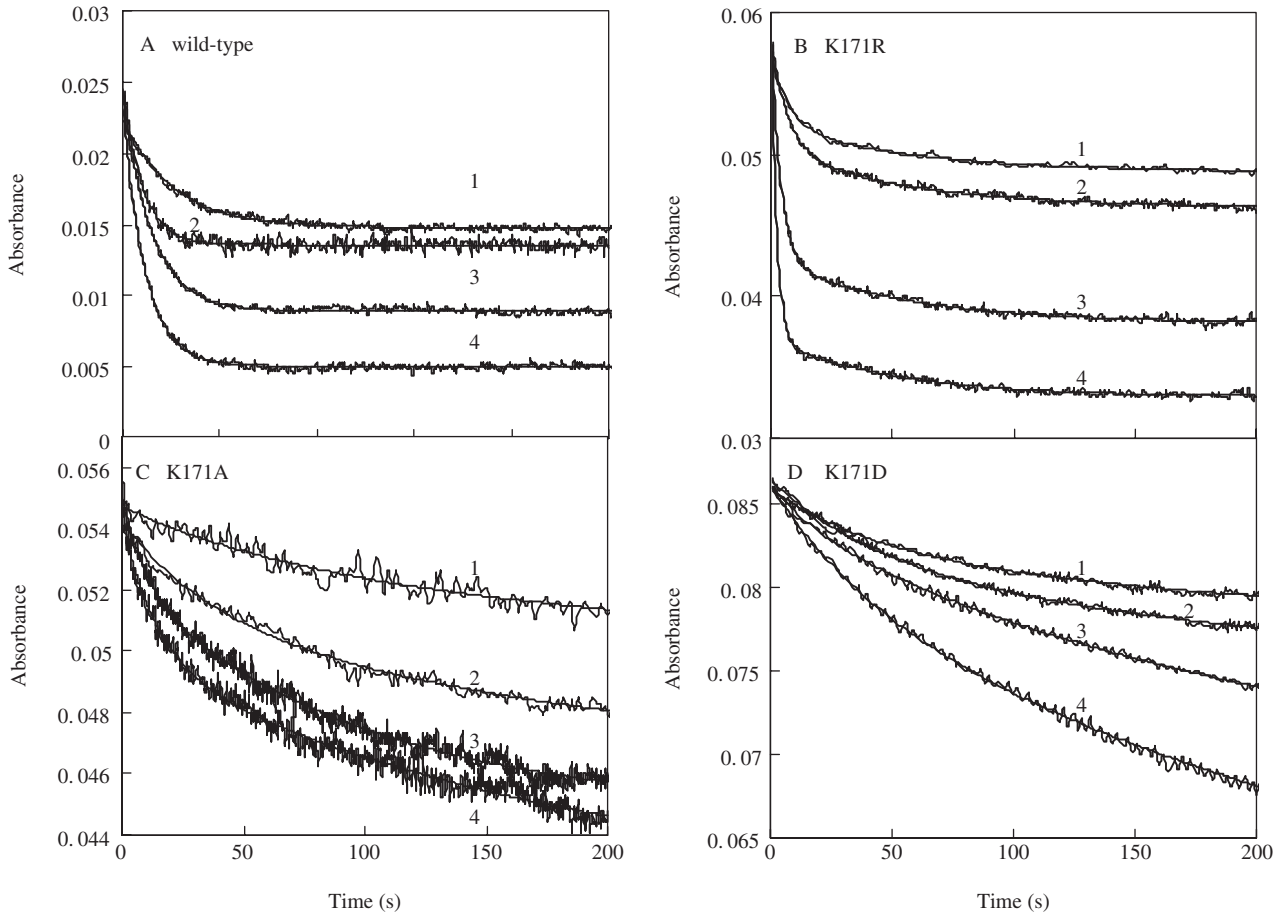

Fig. 10. **Stopped-flow traces at 450 nm after mixing enzyme with sodium sulphite.** Stopped-flow experiments were performed in 20 mM potassium phosphate buffer (pH 8.0) at 25°C. Enzymes used were the wild-type (A), the mutants K171R (B), K171A (C) and K171D (D), and the enzyme concentration was 5 μM. The final concentrations of sodium sulphite were 0.05, 0.10, 0.20, 0.50 mM in A, 0.1, 0.2, 1.0, 2.0 mM in B, 1.0, 2.0, 3.0, 5.0 mM in C and 0.5, 1.0, 3.0, 5.0 mM in D, for curves 1 to 4, respectively. Stopped-flow traces were explained by a single exponential process in A and B, and a double exponential process in C and D as described in the text.

Reactivity of Sodium Sulphite with the Wild-type and K171 Mutant SO-U96—The results presented above showed that the mutation of Lys171 to Arg, Ala and Asp does not inhibit the rates of reduction of the flavin prosthetic groups of enzyme, non-covalent FAD and covalent FMN. This is a quite reasonable result, since our crystallographic structural model of SO-U96 shows that Lys171 places outside the linear path from non-covalent FAD to covalent FMN [(*9*), Fig. 2]. Therefore, the lower activity of K171 mutant enzymes must be derived from the lower reactivity of the reduced FMN with molecular oxygen. Our stopped-flow apparatus is not convenient to measure the rate of oxidation of the stoichiometrically reduced enzyme with oxygen. However, as described above, the dissociation constant of enzyme–sulphite complex is linearly related to $K_m^{O_2}$ (Fig. 4). Therefore, as the second best, we measured the rate of reaction of enzyme with sodium sulphite to represent the reactivity of the reduced FMN with molecular oxygen. The reaction of enzyme with sodium sulphite was followed by monitoring the absorbance change at 450 nm (Fig. 10). Stopped-flow traces were analysed on the basis of the pseudo-first-order reaction, fitting a single exponential process using a software equipped with the apparatus, modifying Equation 1 to a single exponential expression. The k_{obs} values were determined at various concentrations of sodium sulphite, and analysed as described by Fersht (*20*). The reaction of enzyme with sodium sulphite can be expressed:

$$E_{ox} + S_f \underset{k_{-1}}{\overset{k_{+1}}{\rightleftharpoons}} E_{ox} \cdot S_f$$

where E_{ox} and S_f represent the oxidized form of enzyme and sulphite, respectively. The reaction of the enzyme with sulfite can be treated as the pseudo-first-order reaction at sulphite concentrations sufficiently greater than the enzyme concentration. Then, the first-order rate obtained is expressed as Equation 5 (*20*).

$$k_{obs} = k_{+1}[S_f] + k_{-1} \quad (5)$$

where k_{obs} represents the first-order rate constant observed. The absorbance decrease was explained by

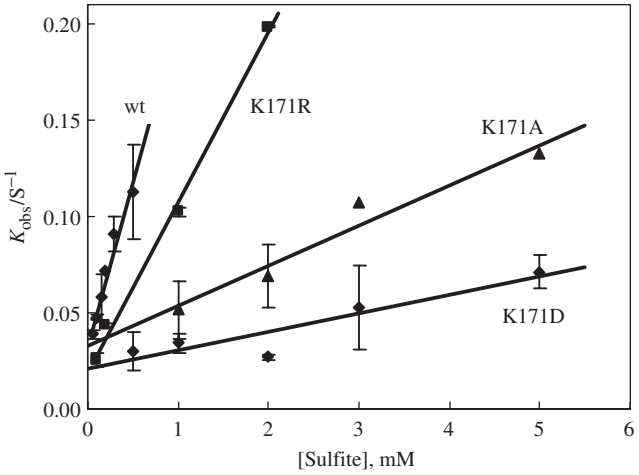

Fig. 11. **The effect of the sodium sulphite on the rates of the reactions with the wild-type and mutant enzymes.** Enzymes were wild-type (A), the mutants K171R (B), K171A (C) and K171D (D).The rates were determined as in Fig. 10. Reaction conditions were described under Fig. 10. From the plots, the rates of association and dissociation were determined as described in the text.

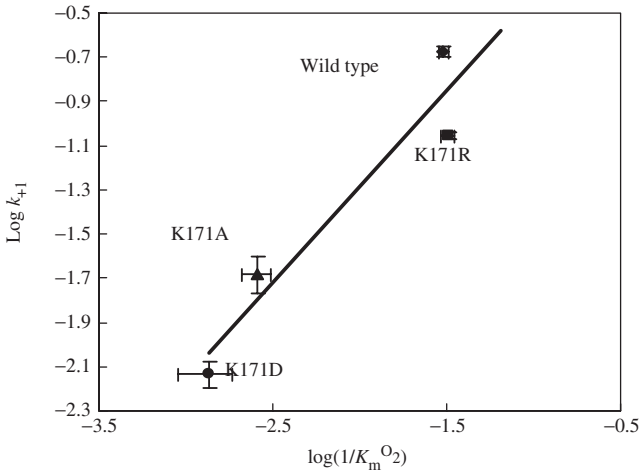

Fig. 12. **Relationship between Logk_{+1} and Log(1/ $K_m^{O_2}$).** The data in Table 1 are used. The rate constant for the formation (k_{+1}) of enzyme–sulphite complex were determined by the stopped-flow method, as described in Fig. 11. The $K_m^{O_2}$ values were determined by measuring oxygen uptake at several concentrations of oxygen, as described in Fig. 1 (B).

two-exponential process for the K171A and K171D mutant enzymes, the faster rate (k_{obs}) was taken. Figure 11 shows a relationship between k_{obs} and sulphite concentration. Finite intercepts on the ordinate were observed and the value obtained was similar in the wild-type and K171 mutant enzymes. The rate constants, k_{+1} and k_{-1} were determined from the plot. Then K_d is calculated by dividing k_{-1} by k_{+1} and shown in Table 1. It is very interesting that the rate of association of sulphite (k_{+1}) with enzyme was largely affected by mutation, but that of dissociation of sulphite from the complex (k_{-1}) was not affected so much. If this can be applied for the association and dissociation of oxygen with enzyme, the rate of association of oxygen is inhibited by the K171 mutation to R, A or D, then a reciprocal of apparent $K_m^{O_2}$ may be assumed to be a function of rate of association of oxygen. Then logk_{+1} was plotted against log (1/$K_m^{O_2}$). A linear relationship was observed as shown in Fig. 12, supporting this assumption. That is, the rate of association of the enzyme with oxygen decreased in the order of the wild-type, K171R, K171A, and K171D mutant enzymes, agreeing with the order of the decrease of the activity of enzyme (Table 1).

DISCUSSION

Chemical modification of SO-U96 by IAM showed that IAM specifically modifies Lys residues of β subunit, K171 and K358 (*6*, *7*), and that K358 presents at sarcosine-binding site (non-covalent FAD-binding site) and K171 at oxygen-binding site (covalent FMN-binding site) (*6*, *7*). We proposed that by IAM-modification of K171 non-covalent FAD mainly functions in the oxidation of sarcosine (*6*). In the present work, to clarify this point and to study further the role of these Lys residues in the catalysis of the enzyme, we produced three mutants for each residues to Arg, Ala and Asp.

As for K358 mutant enzymes, K358A and K358D mutants did not show the enzyme activity, but very low activity was observed with the K358R mutant enzyme (Table 1). The results are quite reasonable, since the carboxy oxygen must bind to ε-amino hydrogen of K358 by the hydrogen bond (*9*), and the side chain of the Ala and Asp residues cannot form the hydrogen bond with the carboxy oxygen of sarcosine. On the other hand, the guanidium group of K358R can form the hydrogen bond, but the bond must not be well-oriented for the carboxy group of sarcosine. Therefore, K358R mutant showed low activity and high K_m for sarcosine (Table 1).

On IAM-modification of K171, the catalytic activity of the modified native SO-U96 decreased to nearly 50% of the native one (*6*). But the enzyme activity of the K171 mutants was different in different mutants. At the saturating concentrations of sarcosine and oxygen, the K171R mutant enzyme showed 60% activity of the wild-type, and K171A and K171D mutants showed nearly 40% activity (Table 1). Moreover, the rate of the FAD reduction in the mutant enzymes was almost identical with that of the wild-type enzyme (Fig. 6). These kinetic properties of the wild-type and K171 mutant enzymes and the 3D structure of the wild-type enzyme (*9*) suggest that our previous proposal (*6*) of the direct path of electron transfer from the reduced FAD to oxygen in the IAM-modified enzyme is not correct.

The rapid reaction kinetics of the reductive-half reaction of the wild-type and K171 mutant enzymes in the presence of sodium sulphite was essentially the same (Fig. 6), suggesting that the reactivity of non-covalent FAD with sarcosine is not affected by the mutation of K171 to R, A or D. This is quite reasonable, since the

Lys residue is located near the covalent FMN and outside of the linear path from FAD to FMN [Fig. 2; (*9*)].

The spectral change monitored by the photodiode array spectroscopy of the wild-type enzyme under anaerobic conditions showed the weak band at 500–700 nm region during reduction with sarcosine (Fig. 7A), indicating the formation of small amounts of neutral semiquinone. Similar result was obtained with the K171R mutant enzyme (Fig. 7B). So, the reductive half-reaction of these enzymes can be expressed by Scheme 3 presented in the 'Results' section. For the analysis of time-dependent absorbance decrease, we assumed that the fast phase is the step of the reduction of the bound FAD to the fully reduced form. We therefore expected that the limiting value of k_{obs1}, $k_{obs1/max}$ is $k_{red/max}$ (145.9 s) obtained in the presence of sodium sulphite. But the value $k_{obs1/max}$ was 59.2 s as shown in Table 2. This must be derived from the fact that at 450 nm we are observing the absorbance decrease due to both FAD and FMN reduction. Therefore, using the software equipped with our stopped-flow apparatus, we fitted the time-dependent absorbance change by fixing k_{obs1} obtained at a given concentration of sarcosine under anaerobic conditions to k_{obs1} at the same concentration of sarcosine in the presence of 40 mM sodium sulphite (Fig. 6), then we can estimate the observed rate constants of steps 2 and 3 to be k_{obs2f} and k_{obs3f}, respectively, where k_{obs2f} and k_{obs3f} are the fitted values obtained. Figure 13 shows a reciprocal plot between the fitted values obtained and sarcosine concentration. The maximum values were determined by extrapolating the k_{obs2f} and k_{obs3f} values obtained at various concentrations of sarcosine to the saturating concentration of sarcosine (Fig. 13, Table 3).

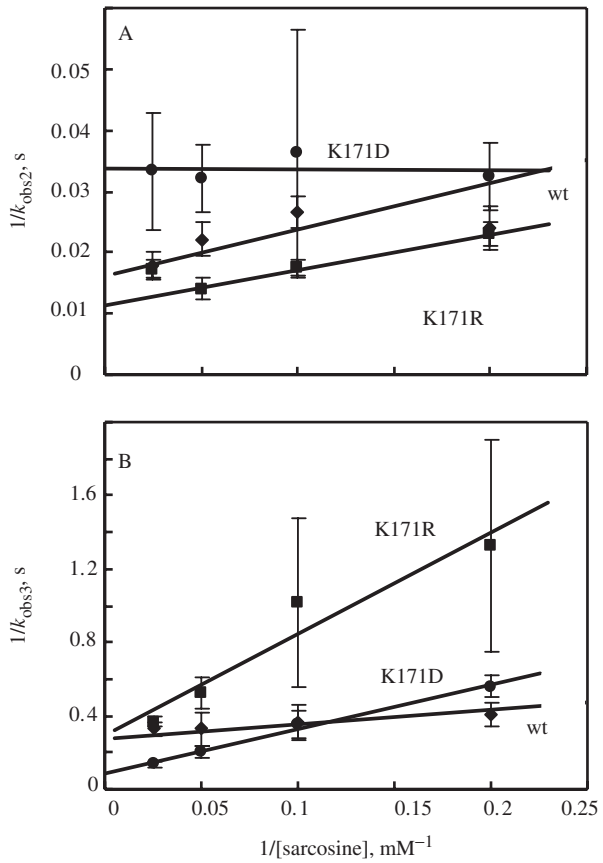

Fig. 13. **Double-reciprocal plot of the observed rate constants (k_{obs1}, k_{obs2}) versus sarcosine concentration.** The stopped flow traces used to determine k_{obs} values in Fig. 8 were fitted to determine the rate constants by fixing k_{obs1f} value to the k_{obs1} value at given concentrations of sarcosine in the presence of sodium sulphite. The k_{obs2f} and k_{obs3f} (A and B) were the respectively fitted values. Enzymes used were wild-type (filled diamond), the mutants K171R (filled square), K171A (filled triangle) and K171D (filled circle).

As for the mechanism of the reductive half-reaction of K171A and K171D mutants, the stopped-flow data can be well explained by Scheme 4. The FAD moiety of the K171A and K171D mutants was rapidly reduced to form the fully reduced FAD, then changes to the semiquinoid form, and finally the semiquinoid form disappears very slowly. This explains the formation of a long-wavelength species during reduction (Fig. 7). The observed maximum rate of reduction, $k_{obs1/max}$, 121.6 s for K171A is quite similar to $k_{red/max}$(145.9 s). But $k_{obs1/max}$ (76.7 s) for K171D is half of the value $k_{red/max}$ (145.9 s). Therefore, we fitted a time-dependent absorbance change of K171D mutant enzyme at given concentration of sarcosine by fixing the k_{obs1} value obtained under anaerobic conditions to k_{obs1} value obtained at the same sarcosine concentration in the presence of sodium sulphite (Fig. 6) as described for the wild-type and K171R mutant enzymes. The stopped-flow trace was well-fitted by three-exponential expression. Using k_{obs} values obtained, we determined the maximum value of k_{obs}, $k_{obsf/max}$ (Fig. 13, Table 3).

Combining the results in Table 3 with those in Table 2, the mechanism of the reductive half-reaction of the enzyme appears. As for the reductive half-reaction of the wild-type and K171R mutant enzymes, the observed rate constant ($146\ s^{-1}$) of the fast face is the step to form the reduced FAD, that ($60\ s^{-1}$ for the wild-type, and $72\ s^{-1}$ for the K171R) of the intermediate face to form the oxidized FAD and the fully reduced form of FMN moieties, and that ($3.6\ s^{-1}$ for the wild-type and $3.4\ s^{-1}$ for K171R) of the

Table 3. **Kinetic parameters obtained by fixing the rate of reduction of the FAD moiety of enzyme to k_{obs1}.**

Enzyme	$k_{obs1f/max}$ (s^{-1}) ($K_{d/obs1}$ [mM])[b]	$k_{obs2f/max}$ (s^{-1}) ($K_{d/obs2}$ [mM])[b]	$k_{obs3f/max}$ (s^{-1}) ($K_{d/obs3}$ [mM])[b]
wild-type	145.9 ± 5.3 (11.9 ± 0.82)	59.9 ± 2.9 (3.24 ± 0.54)	3.63 ± 0.22 (2.35 ± 0.57)
K171R	145.9 ± 5.3 (11.9 ± 0.82)	72.0 ± 3.4 (2.79 ± 0.59)	3.42 ± 0.54 (12.4 ± 4.04)
K171A	121.6 ± 9.7 (11.2 ± 1.9)	22.6 ± 1.6 (n.d.)	4.40 ± 0.88 (n.d.)
K171D	145.9 ± 5.3 (11.9 ± 0.82)	35.9 ± 2.0 (n.d.)	14.3 ± 1.6 (34.5 ± 5.6)

The time-dependent absorbance change at 450 nm was fitted as described in the text by fixing k_{obs1} value to be that obtained in the presence of sodium sulphite (Fig. 6) except the K171A mutant (see DISCUSSION). The value for K171A is the value in Table 2.

slow face to form the fully reduced forms. As for the reductive half-reaction of K171A and K171D mutants, $k_{obs2f/max}$ (Table 3) agrees well with the observed rate constant of the appearance of long wavelength intermediate ($k_{obs1/max}$ in Table 2), then these values must be the observed rates of formation of the semiquinoid species. Similar consideration will be applied to $k_{obs2f/max}$ (Table 3) and $k_{obs1/max}$ (Table 2). Then, the reductive half-reaction of wild-type, K171R, K171A and K171D mutant enzymes can be written by introducing the observed rate constants in the Scheme 5. In Scheme 4, the semiquinoid species directly reacts with sarcosine for K171A and K171D mutants, but the oxidized form of FAD reacts with sarcosine in Scheme 5, since it seems reasonable that sarcosine reacts with the oxidized FAD.

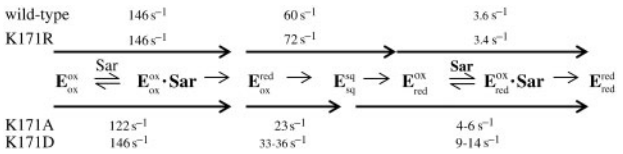

Scheme. 5. A possible mechanism of reductive half-reaction of the wild-type and mutant enzymes. The observed rate constants for the wild-type and K171smutant enzymes are shown.

In the above discussion, the properties of the semiquinoid species is not mentioned. There are so-called 'diflavin enzyme family', such as NADPH-cytochrome P450 reductase (CPR) and nitric oxide synthase reductase [see (*21*) for review], L-proline dehydrogenase (PDH) (*22*) and tetrameric SOs (*1*, *14*, *17*, *19*, *23*). Moreover, there are a series of works on the oxidation-reduction properties of flavodoxin (*24–30*) and on the 8α-imidazoyle-substituted flavins (*31*, *32*). Making reference to these works, we like to consider the semiquinoid species observed with the wild-type and K171mutant SO-U96, and SO-P1.

During the reductive half-reaction, K171A and K171D mutants of SO-U96 showed characteristic spectra of the neutral and anionic semiquinones. Similar semiquinoid species were observed with SO-P1 (*14*, *19*). Chen *et al*. (*23*) proposed the following reactions from their structural analyses of SO from *Pseudomonas maltophilia* (SO-MAL) by the assumption that the reduction of flavins of SO-MAL proceeds by the steps proposed for the enzyme SO-P1:

$$FADH^- + FMN \rightarrow FADH^{\cdot} + FMN^{\cdot -}$$
$$FADH^{\cdot} + FMN^{\cdot -} \rightarrow FAD + FMNH^-$$

The fully reduced state of the FAD prosthetic group is postulated to be anionic, and one electron transfer produces neutral $FADH^{\cdot}$ and anionic $FADH^{\cdot -}$ semiquinones (*23*). As for K171A and K171D mutants of SO-U96, spectral changes during reduction suggest the formation of neutral and anionic semiquinones, and the above scheme by Chen *et al*. (*23*) can be applied for the formation of semiquinones. As for the wild-type and K171R mutant enzymes, we did not detect clearly the semiquinoid species during reduction. But we could not completely deny the formation of semiquinoid species because of small change of absorbance at 500–700 nm region (Fig. 7A). In addition to this, the primary structure between SO-U96 and SO-P1 are highly homologous, this fact suggests that the structure around flavin rings is quite similar between SO-U96 and SO-P1. Therefore, we postulated in the above scheme that the wild-type and K171R mutant enzymes also form the biradical forms during reduction. Then, why semiquinoid forms were observed with SO-P1, K171A and K171D mutants, but not so much with the wild-type and K171R mutant enzymes.

The redox potentials of flavin cofactors are regulated by interactions between the cofactors and its apoproteins. The short and long-range electrostatic, π–π aromatic stacking, and hydrogen-bonding interactions have been demonstrated for flavodoxins (*24–30*). The strength of hydrogen-bonding interaction between the carbonyl group of Gly57 and the proton on N(*5*) of neutral semiquinone radical is dependent on the properties of the side chain at position of 57 (*29*, *30*). Moreover, it has been suggested that the redox properties of enzyme containing the 8α-histidyl-substitued flavin are modulated by the ionization of imidazole ring (*31*, *32*). From these reports, there may be several possibilities to account for the spectral (semiquinoid) species observed during reduction in our enzymes and others. First, the FMN cofactor of SO-U96 is covalently bound with His172, therefore it is possible that the mutation of Lys171 to non-ionic Ala or anionic Asp might change the ionization of His172 to induce the change in the redox state of FMN ring. Then we observed semiquinoid species with the K171A and K171D mutants, but not so clearly with the wild-type and K171R mutant enzymes. Secondly, in the 3D structure of SO-U96 (pdb 1X31), the nearest residue to N(5) of the FMN ring is the side chain carbonyl of Glu270 (3.16 Å). It is, therefore, possible that the interaction between them might be different among SO-U96, its K171 mutants and SO-P1. At last, as the length between the 2′-hydroxyl of the ribityl O(2′) side chain and N(1) of the FMN ring is estimated to be 2.48 Å(pdb 1X31), there might be an interaction of the 2′-hydroxyl of the ribityl side chain with N(1) of the flavin ring, and this interaction might be affected by a slight conformational change surrounding the ribityl side chain. In these possibilities, we postulate that the ionization difference of imidazole ring of H172 might be the most likely reason to induce the difference in the stability of neutral semiquinone between the wild-type (or K171R) and K171A(or K171D) mutant enzymes, since K171 is adjacent residue of H172. Further works on the 3D structural analyses of the sarcosine-reduced SO-U96, and of the oxidized and sarcosine-reduced forms of K171A or K171D mutant enzymes are required. However, the difference in the stability of neutral semiquinone between SO-U96 and SO-P1 is still difficult to explain. As will be discussed subsequently, the difference might stem from the SO-P1 preparations containing 30% inactive enzyme (*14*, *19*).

The observed rate constants of the wild-type and K171 mutant enzymes (Tables 2, 3 and Scheme 4) clearly show that the reductive-half reaction is not inhibited by the mutation of K171 to R, A or D. It is therefore concluded

Table 4. **Comparison of kinetic perameters of Corynebacterial enzymes.**

Origin		k_{cat} (s^{-1})	K_m(Sarcosine) (mM)	Km(O_2) (μM)	Φ_1, Ms	Φ_2, Ms	Temperature (°C)	Reference
sp.U-96	native	18	3.3	52	1.83×10^{-4}	2.88×10^{-6}	25	Kawamura-Konishi & Suzuki(1987)
	native	16.7	2.1	25			30	Hayashi *et al.*(1983)
	wild-type	18.0	2.8	17.6			25	Present results
sp. P-1	native	42.5	5.37	636	1.26×10^{-4}	1.49×10^{-5}	25	Ali *et al.*(1991)

The kinetic parameters refered above were obtained from the rate data by measuring the oxygen uptake at pH 8.0. Φ_1 and Φ_2 are the kinetic paprmeters according to Dalziel (*39*). $\Phi_1, = K_{sarcosine}/k_{cat}$; $\Phi_2 = K_{oxygen}/k_{cat}$, here K is the dissociation constant of enzyme–sarcosine or enzyme–oxygen complex.

that the low activity observed with K171R, K171A and K171D mutants (Table 1) is derived from the inhibition of oxidation of the reduced FMN with oxygen, though we did not determine the rate of oxidation of the reduced FMN with oxygen. However, the rate constants of binding of sulphite with the FMN moiety of enzyme support this conclusion (Table 1, Fig. 12).

At pH 8.0, the amino group of K171 is protonated, since p*K*a of the group is 8.7(7). From the outside of SO-U96 molecule, molecular oxygen must diffuse to the FMN ring through the tunnel (Fig. 2). K171 and K277 face the tunnel near the flavin ring. The presence of cationic side chain near the flavin ring images us the structure of oxygen-binding to heme in hemoglobin. In hemoglobin, the distal His residue supports the fine orientation of molecular oxygen to heme iron (*33*). We suppose that K171 and possibly K277 may have a role like the distal His in hemoglobin. It is conceivable that the electron negative oxygen must be caught by these Lys residues to oxidize the reduced FMN. The oxidase flavin may have the cationic residue like K171 near the flavin ring, though Mattevi's (*34*) recent review describes that there are no structural rules to enable prediction of whether or how a flavoenzyme reacts with oxygen. There are oxidases such as glucose oxidase (*35*), cholesterol oxidase (*36*) and xanthine oxidase (*37*), which the presence of the positive charge in the active site enhances the oxygen reactivity (*34*). It is possible that the reactivity of the reduced FMN (semiquinone and/or fully reduced) with molecular oxygen might be affected by the ionic state of the FMN moiety. At present, however, how the mutation of Lys171 to Ala and Asp affects the ionic state of FMN ring is difficult to see as mentioned earlier. To study the oxygen reactivity of flavoenzymes, heterotetrameric SO, like SO-U96, SO-P1 and SO-ART may be a good model enzyme, since the enzyme FMN specifically reacts with oxygen, but not with sarcosine.

There were some discussion on the mechanism of the reductive half-reaction of the corynebacterial enzymes, SO-U96 and SO-P1. As for the reductive titration and reductive half-reaction experiments on the SO-U96 (*12*, *38*), a possible contamination of oxygen during experiments was pointed by the workers on SO-P1, and the difference in the mechanism of reductive half-reaction between SO-U96 and SO-P1 was suggested to stem from the oxygen contamination (*14*, *19*). The point is that during reduction of enzyme with sarcosine, the semiquinoid form was observed with SO-P1 (*14*, *19*), but not with SO-U96 (*12*, *38*). Therefore, in the present work, we performed the stopped-flow reductive-half reaction very carefully. The small and broad band observed at 500–700 nm region during the anaerobic reduction with sarcosine (Fig. 7A) may be the reason that the spectra suggesting the presence of neutral semiquinone were not observed in the previous works on SO-U96 (*12*, *38*). Workers of SO-P1 also claimed that they observed almost the same kinetic results by their side-by-side studies of SO-U96 and SO-P1 (*19*). This means that they got kinetic parameters of SO-U96 to be those of SO-P1 as summarized in Table 4. That is, SO-U96 they used must have 12–25 times higher apparent $K_m^{O_2}$ than SO-U96 that we used, since an apparent $K_m^{O_2}$ of SO-P1 is more than 12–25 times higher than that of SO-U96 that we used (Table 4). It is possible that SO-U96 they used was partially denatured to show a low $K_m^{O_2}$ (*14*, *19*). Anyhow, the difference in kinetic behaviour between SO-P1 and SO-U96 (Table 4) means that the affinity of the reduced FMN species (fully reduced or semiquinoid form) of SO-P1 with oxygen is lower than that of SO-U96.

The kinetic behavior of SO-P1 is quite similar to that of the K171D mutant of SO-U96, but not to the wild-type and K171R enzymes. That is, the K171D mutant has an apparent $K_m^{O_2}$ similar to that of SO-P1 (Table 1), and shows the semiquinoid species during the reductive-half reaction (Fig. 7D). Therefore, the conformation around the covalent FMN of SO-P1 must be quite similar to that of the K171D mutant. Though SO-U96 and SO-P1 were both derived from *Corynebacterium*, they catalyse the SO reaction by a similar but not identical mechanism.

Authors are indebted to their colleague Dr Y. Kawamura-Konishi, now Ishikawa Pref. Univ., for her valuable discussion during the course of this work. Authors are also indebted to Prof. N.Makino, Ibaraki Pref. Univ. of Health Sciences for his critical reading of manuscript.

REFERENCES

1. Suzuki, H. (1994) Sarcosine oxidase: structure, function, and the application to creatinine determination. *Amino Acids* **7**, 27–43
2. Suzuki, M. (1981) Purification and some properties of sarcosine oxidase from *Corynebacterium* sp. U-96. *J. Biochem.* **89**, 599–607
3. Kvalnes-Krick, K. and Jorns, M.S. (1986) Bacterial sarcosine oxidase: comparison of two multisubunit enzymes containing both covalent and noncovalent flavin. *Biochemistry* **25**, 6061–6069
4. Ogushi, S., Nagano, K., Emi, S., Ando, M., and Tsuru, D. (1988) Sarcosine oxidase from *Arthrobacter ureafaciens*: purification and some properties. *Chem. Pharm. Bull.* **36**, 1445–1450

5. Meskys, R., Rudomanskis, R., and Leipuviene, R. (1996) Cloning of genes encoding heterotetrameric sarcosine oxidase from *Arthrobacter* sp. *Biotech. Lett.* **18**, 781–786
6. Suzuki, H. and Kawamura-Konishi, Y. (1991) Cysteine residues in the active site of *Corynebacterium* sarcosine oxidase. *J. Biochem.* **109**, 909–917
7. Mukouyama, E.B., Oguchi, M., Kodera, Y., Maeda, T., and Suzuki, H. (2004) Low pKa lysine residues at the active site of sarcosine oxidase from *Corynebacterium* sp.U-96. *Biochem. Biophys. Res. Commn.* **320**, 846–851
8. Suzuki, H., Tamamura, R., Yajima, S., Kannno, M., and Suguro, M. (2005) *Corynebacterium* sp. U-96 contains a cluster of genes of enzymes for the catabolism of sarcosine to pyruvate. *Biosci. Biotechnol. Biochem.* **69**, 952–956
9. Ida, K., Moriguchi, T., and Suzuki, H. (2005) Crystal structure of heterotetrameric sarcosine oxidase from Corynebacterium sp. U-96. *Biochem. Biophys. Res. Commn.* **333**, 359–366
10. Moore, J.T., Uppal, A., Maley, F., and Maley, G.F. (1993) Overcoming inclusion body formation in a high-level expression system. *Protein Express. Purif.* **4**, 160–163
11. Ausbel, F., Brent, R., Kingston, R.E., Moore, D.D., Seidman, J.G., Smith, J.A., and Struhl, K. (1995) *Short Protocols in Molecular Biology* 3rd edn. John Wiley & Sons, Inc
12. Kawamura-Konishi, Y. and Suzuki, H. (1987) Kinetic studies on the reaction mechanism of sarcosine oxidase. *Biochim. Biophys. Acta* **915**, 346–356
13. Jorns, M.S. (1985) Properties and catalytic function of the two nonequivalent flavins in sarcosine oxidase. *Biochemistry* **24**, 3189–3194
14. Zeller, H.-D., Hille, R., and Jorns, M.S. (1989) Bacterial sarcosine oxidase: identification of novel substrates and a biradical reaction intermediate. *Biochemistry* **28**, 5145–5154
15. Müller, F. and Massey, V. (1969) Flavin-sulfite complexes and their structures. *J.Biol.Chem.* **244**, 4007–4016
16. Massey, V., Müller, F., Feldbeg, R., Schuman, M., Sullivan, P.A., Howell, L.G., Mayhew, S.G., Matthews, R.G., and Foust, G.P. (1969) The reactivity of flavoproteins with sulfite. Possible relevance to the problem of oxygen reactivity. *J. Biol. Chem.* **244**, 3999–4006
17. Harris, R.J., Meskeys, R., Sutcliffe, M.J., and Scrutton, N.S. (2000) Kinetic studies of the mechanism of carbon-hydrogen bond breakage by the heterotetramertic sarcosine oxidase of *Arthrobacter* sp. 1-IN. *Biochemistry* **39**, 1189–1198
18. Michaelis, L. (1951) Theory of oxidation-reduction in *The Enzyme, Chemistry and Mechanism of Action.* pp.1–52
19. Ali, S.N., Zeller, H.-D., Calisto, M.K., and Jorns, M.S. (1991) *Biochemistry* **30**, 10980–10986
20. Fersht, A. (1998) *Structure and Mechanism in Protein Science.* p.143 W.H. Freeman and Company, USA
21. Iyanagi, T. (2005) Structure and function of NADPH-cytochrome P450 reductase and nitric oxide synthase reductase domain. *Biochem. Biophys. Res. Commn.* **338**, 520–528
22. Tsuge, H., Kawakami, R., Sakuuraba, H., Ago, H., Miyano, M., Aki, K., Katunuma, N., and Ohshima, T. (2005) . *J. Biol. Chem.* **280**, 31045–31049
23. Chen, Z.-W., Hassan-Abdulan, A., Zhao, G., Jorns, M.S., and Mathews, F.S. (2006) Heterotetrameric sarcosine oxidase: structure of a diflavin metalloenzyme at 1.85 Å resolution. *J. Mol. Biol.* **360**, 1000–1018
24. Zhou, Z. and Swenson, R.P. (1995) Electrostatic effects of surface amino acid residues on the oxidation-reduction potentials of the flavodoxin from *Desulfovibrio vulgaris* (Hildenborough). *Biochemistry* **34**, 3183–3192
25. Swenon, R.P. and Krey, G.D. (1994) Site-directed mutagenesis of tyrosine-98 in the flavodoxin from *Desulfovibrio vulgaris* (Hildenborough): regulation of oxidation-reduction properties of the bound FMN cofactor by aromatic, solvent, and electrostatic interactions. *Biochemistry* **33**, 8505–8514
26. Chang, F.C. and Swenson, R.P. (1997) Regulation of oxidation-reduction potentials through redox-linked ionization in the Y98H mutant of the *Desulfovibrio vulgaris* (Hildenborough) flavodoxin: direct proton nuclear magnetic resonance spectroscopic evidence for the redox-dependent shift in the p*K*a of Histidine-98. *Biochemistry* **36**, 9013–9021
27. Bradley, L.H. and Swenson, R.P. (1999) Role of glutamate-59 hydrogen bonded to N(3)H of the flavin mononucleotide cofactor in the modulation of the redox potentials of the *Clostridium beijerinckii* flavodoxin. Glutamate-59 is not responsible for the pH dependency but contributes to the stabilization of the flavin semiquinone. *Biochemistry* **38**, 12377–12386
28. Bradley, L.H. and Swenson, R.P. (2001) Role of hydrogen bonding interactions to N(3)H of the flavin mononucleotide cofactor in the modulation of the redox potentials of the *Clostridium beijerinckii* flavodoxin. *Biochemistry* **40**, 8686–8695
29. Ludwig, M.L., Pattridge, K.A., Metzger, A.L., Dixon, M.M., Eren, M., Feng, Y., and Swenson, R. (1997) Control of oxidation-reduction potentials in flavodoxin from *Clostridium beijerinckii*: the role of conformational changes. *Biochemistry* **36**, 1259–1280
30. Chang, F.C. and Swenson, R.P. (1999) The midpoint potentials for the oxidized-semiquinone couple for Gly57 mutants of the *Clostridium beijerinckii* flavodoxin correlate with changes in the hydrogen-bonding interaction with the proton on N(5) of the reduced flavin mononucleotide cofactor as measured by NMR chemical shift temperature dependencies. *Biochemistry* **38**, 7168–7176
31. Williamson, G. and Edmondson, D.E. (1985) Effect of pH on oxidation-reduction potentials of 8α-*N*-imidazole-substituted flavins. *Biochemistry* **24**, 7790–7797
32. Williamson, G. and Edmondson, D.E. (1985) Proton nuclear magnetic resonance studies of 8α-*N*-imidazolylriboflavin in its oxidized and reduced forms. *Biochemistry* **24**, 7918–7926
33. Perutz, M.F. (1989) Myoglobin and hemoglobin: role of distal residues in reactions with haem ligands. *Trends Biochem. Sci.* **14**, 42–44
34. Mattevi, A. (2006) To be or not to be an oxidase: challenging the oxygen reactivity of flavoenzymes. *Trends Biochem. Sci.* **31**, 276–283
35. Roth, J.P. and Klinman, J.P. (2003) Catalysis of electron transfer during activation of O_2 by the flavoprotein glucose oxidase. *Proc. Natl. Acad. Sci. USA* **100**, 62–67
36. Coulombe, R., Yue, K.Q., Ghisla, S., and Vrielinsk, A. (2001) Oxygen access to the active site of cholesterol oxidase through a narrow channel is gated by an Arg-Glu pair. *J. Biol. Chem.* **276**, 30435–30441
37. Enroth, C., Eger, B.T., Okamaoto, K., Nishino, T., Nishino, T., and Pai, E. (2000) Crystal structures of bovine milk xanthine dehydrogenase and xanthine oxidase: structure-based mechanism of conversion. *Proc. Natl. Acad. Sci. USA* **97**, 10723–10728
38. Hayashi, S. (1984) Mechanism of reduction of *Corynebacterium* sarcosine oxidase by dithiothreitol. *J. Biochem.* **95**, 1201–1207
39. Dalziel, K. (1969) The interpretation of kinetic data for enzyme-catalyzed reactions involving three substrate. *Biochem. J.* **114**, 547–556